

Synergistic action of advanced glycation end products and endogenous nitric oxide leads to neuronal apoptosis in vitro: A new insight into selective nitroergic neuropathy in diabetes

S. Cellek¹ · W. Qu² · A. M. Schmidt² · S. Moncada¹

¹ Wolfson Institute for Biomedical Research, University College London, London, UK

² Department of Surgery, College of Physicians & Surgeons, Columbia University, New York, New York, USA

Abstract

Aims/hypothesis. We have previously shown that in diabetes nitroergic neurones innervating the urogenital and gastrointestinal organs undergo a selective degenerative process. This comprises an initial insulin-reversible decrease in neuronal nitric oxide synthase (nNOS) in the axons, followed by apoptosis of the nitroergic neurones, a process that is not reversible by insulin. Since apoptosis was independent of serum glucose concentrations, and advanced glycation endproducts (AGEs) have been implicated in the pathogenesis of diabetic complications, we have now measured AGEs in the serum and penis, pyloric sphincter and pelvic ganglia of diabetic animals at different times after streptozotocin treatment. Furthermore, we have studied their effect in vitro on human neuroblastoma (SH-SY5Y) cells in the presence or absence of nNOS expression.

Methods. Serum AGEs were measured using fluorometry and ELISA. Accumulation of AGEs in the tissues was evaluated with immunohistochemistry. The viability, apoptosis and oxidative stress in SH-SY5Y

cells were measured upon exposure to AGEs or high concentrations of glucose.

Results. AGEs increased gradually in the serum and tissues of streptozotocin-induced diabetic rats; this process was not affected by delayed insulin treatment. In SH-SY5Y cells, AGEs, but not high glucose concentrations, increased the reactive oxygen species and caspase-3-dependent apoptosis in a synergistic fashion with endogenous nitric oxide (NO). Apoptosis was prevented by treatment with a NOS inhibitor, a pan-caspase inhibitor, a soluble receptor of AGEs or an anti-oxidant, but not an inhibitor of soluble guanylate cyclase.

Conclusions/interpretation. The synergistic actions of NO and AGEs account for the irreversible nitroergic degeneration in diabetes. [Diabetologia (2004) 47: 331–339]

Keywords Diabetes mellitus · Nitric oxide · Advanced glycation endproducts · Oxidative stress · Apoptosis · Autonomic neuropathy · Neurodegeneration · Nitroergic

Received: 21 July 2003 / Revised: 2 October 2003

Published online: 16 December 2003

© Springer-Verlag 2003

S. Cellek (✉)

Wolfson Institute for Biomedical Research,
University College London, Gower Street,
Cruciform Building, London, WC1E 6BT, UK
E-mail: s.cellek@ucl.ac.uk

Abbreviations: AGEs, advanced glycation endproducts · eNOS, endothelial nitric oxide synthase · HSA-AGEs, advanced glycated human serum albumin · iNOS, inducible nitric oxide synthase · L-NAME, N^G-nitro-L-arginine methyl ester (NOS inhibitor) · MPG, major pelvic ganglion; NAC, N-acetyl-L-cysteine · NO, nitric oxide · NOS, nitric oxide synthase · nNOS, neuronal nitric oxide synthase · ODQ, 1H-[1,2,4]oxadiazolo[4,3,-a] quinoxalin-1-one (sGC inhibitor) · RA, retinoic acid · ROS, reactive oxygen species · sRAGE, soluble receptor of advanced glycation endproduct · STZ, streptozotocin · Z-VAD-FMK, Z-Val-Ala-Asp(OMe)-CH₂F (pan-caspase inhibitor)

Diabetic autonomic neuropathy can lead to diabetic gastropathy, erectile dysfunction and female sexual dysfunction which are due to impairment in the function of nitric oxide (NO)-generating (nitroergic) nerves [1, 2, 3, 4, 5, 6, 7]. Previous studies have shown decreased neuronal NO synthase (nNOS) content in the pylorus and penis of diabetic animals and patients [4, 5, 8, 10, 11, 12, 13, 14]. However, until recently it was not clear whether this decrease was due to degeneration of nitroergic nerves [4] or down-regulation of nNOS protein expression [5, 15]. We have recently shown that [16] nitroergic neurones innervating the penis and gastric pylorus of diabetic rats go through a degenerative process in two phases: in the first phase the neuronal nitric oxide synthase (nNOS) content is decreased in the axons, but not in the cell bodies; this phase is reversible by insulin treatment and is not associated with neurodegenerative changes. In the second phase the neurones undergo an apoptotic degener-

ative process and lose their nNOS content completely; this phase is irreversible by insulin treatment. Nitroergic responses are lost gradually throughout the two phases; this process is reversible by insulin treatment in the first but not in the second phase [16]. Interestingly in the second phase irreversible nitroergic degeneration as well as loss of nitroergic function occur even when the animals are made euglycaemic by treatment with insulin [16]. These findings prompted us to study factors other than high glucose that might lead to apoptotic neurodegeneration.

There is increasing evidence for a role for advanced glycation endproducts (AGEs) in the development of diabetic complications [17]. An AGE-modified form of human haemoglobin has been shown to decline following insulin treatment more slowly than HbA_{1c}, suggesting an irreversible nature of the AGE products [18]. More recently, delayed insulin treatment has been shown to fail to normalise the elevated serum AGE concentrations in diabetic rats [19]. We have therefore measured AGEs in the serum and tissue of diabetic rats with or without insulin treatment. We have also studied the effects of high glucose and AGEs on SH-SY5Y human neuroblastoma cells in the presence or absence of nNOS expression.

Materials and methods

Induction of diabetes. Male Wistar rats (225–250 g) were treated with STZ (75 mg/kg, i.p.) or vehicle (saline) as described previously [4, 16]. Hyperglycaemia was defined as a non-fasting blood glucose concentration over 20 mmol/l. Insulin was administered 4, 8 or 12 weeks after STZ injection using sustained-release insulin rods (~2 U/day; LinBit, Ontario, Canada). Rats were killed at 4, 8, 12, 16 and 20 weeks after STZ injection and their blood, penis, stomach with gastric pylorus and bilateral major pelvic ganglia (MPG) were collected. Blood was centrifuged to obtain serum for measuring AGEs and glucose. All animal experiments were conducted according to the rules outlined by the Home Office, Animals (Scientific Procedures) Act 1986 (project number: 70/05161).

Throughout the paper STZ-treated animals without any insulin replacement are referred as Xw, where X is the number of weeks the animal was kept alive following STZ treatment. STZ-treated animals with insulin replacement are referred as X/Y where X is the number of weeks the animal was kept alive and Y is the number of weeks it received insulin. Insulin treatment was always given for the last Y weeks of the study.

Measurement of AGEs in the serum using fluorometry. AGEs were measured in the whole serum as described previously [20, 21]. The samples were run through a HPLC to measure fluorescence ($\lambda_{\text{ex}}=370$ nm, $\lambda_{\text{em}}=440$ nm) and to measure peptides ($\lambda=214$ nm). AGEs-fluorescence was expressed as the ratio of the area under the fluorescent curve to the area under the peptide curve.

Measurement of AGEs in the serum using ELISA. The wells (96-well Maxisorp ELISA plate, NUNC, Paisley, UK) were coated with polyclonal anti-AGE antibody (AGE102; 10 $\mu\text{g/ml}$; Biologo, Kronshagen, Germany) in 50 mmol/l carbonate buffer (pH 9.6) overnight at room temperature. The

wells were then washed with PBS containing 0.05% Tween 20 and blocked at room temperature with PBS containing 0.25% bovine serum albumin. After washing, the wells were incubated with the standards (AGE-human serum albumin as described below; diluted 1:10–1:100,000) or samples (rat serum diluted in PBS 1:10–1:10,000) at room temperature for 3 h. After washing, the wells were incubated with monoclonal anti-AGE antibody (clone 6D12; 0.5 $\mu\text{g/ml}$; Biologo) for 2 h at room temperature followed by anti-mouse IgG-HRP (1:7500; Autogen Bioclear, Calne, UK) for 1 h at room temperature. The wells were washed again and developed with peroxidase substrate (Autogen Bioclear). The absorbance at 650 nm was measured after a 20 min reaction time. After adding the stopping solution (Autogen Bioclear) the reading was repeated at 450 nm. The absorbance obtained using AGE-human serum albumin was used as standard. Because of the high inter-assay variability the results were expressed as the percentage of the control (non-diabetic) rat serum within the same plate.

Immunostaining of penis, pyloric sphincter and MPG with AGE antibody. After fixation in 4% paraformaldehyde overnight at room temperature, the tissues were transferred into 30% sucrose in phosphate buffer and kept at 4°C overnight. The samples were then frozen in OCT compound (BDH, Poole, UK) and serial cryosections at 10–20 μm intervals were obtained using a cryostat (–18°C; Leica, 2800 Frigocut-E, Bensheim, Germany). The sections were dried on gelatine-coated slides for 2 h at room temperature, then incubated with PBS containing 0.1% Triton X-100 and 5% of the serum of the species from which the secondary antibody was obtained. Then the slides were incubated with antibodies against nNOS (raised in sheep, K205 [22]; 1:2000) or tyrosine hydroxylase (TH; 1:200; Chemicon, Harrow, UK) at 4°C overnight and with advanced glycation endproducts (AGEs; clone 6D12; 2 $\mu\text{g/ml}$; Biologo) for 2 h at room temperature followed by detection with appropriate fluorescent conjugated secondary antibodies. The images were obtained using a laser-scanning confocal microscope (Leica TCS-DMRE, Bensheim, Germany). Image analysis was performed using Leica Confocal Software (Version 2.00, build0871).

The immunostaining density was measured as the mean amplitude of fluorescence per 1 μm^2 in selected areas occupied by nerve cell bodies. In order to avoid day-to-day variation in fluorescence intensity, several sections from different experimental groups were immunostained and analysed in the same batch on the same day. The laser intensity and gain functions were set according to the control tissue; thereafter these settings were applied to all sections from all experimental groups within the same batch. The results were expressed as percentage of control to avoid the variation between different batches.

Production of HSA-AGEs. Human serum albumin (HSA; 50 mg/ml) was incubated with 1 mol/l glucose in PBS in sterile conditions at 37°C for 12 weeks. Excess unbound glucose was then removed using dialysis against a high volume of PBS.

Stimulation of SH-SY5Y cells. Human neuroblastoma cells (SH-SY5Y from European Cell Culture Collection; passages 13–20) were grown in DMEM/F12 mix (1:1) with glutamax-I (Life Technologies, Paisley, UK), 15% foetal calf serum, 10 mmol/l HEPES, 1% non-essential aminoacids and 1% antibiotics. Serum was withdrawn 24 h before any stimulation. The cells were stimulated with retinoic acid (RA; 25 $\mu\text{mol/l}$) and/or HSA-AGEs (0.5 mg/ml) or high glucose (up to 50 mmol/l) in the presence of 0.5% serum and in the absence or presence of an inhibitor of nitric oxide synthase N^G-nitro-L-arginine methyl ester (L-NAME;

500 $\mu\text{mol/l}$), the pan-caspase inhibitor Z-Val-Ala-Asp(OMe)-CH₂F (Z-VAD-FMK; 50 $\mu\text{mol/l}$), the anti-oxidant N-acetyl-L-cysteine (NAC; 100 $\mu\text{mol/l}$), the soluble receptor of AGE (sRAGE; 125 $\mu\text{g/ml}$) or the soluble guanylyl cyclase inhibitor 1H-[1,2,4]oxadiazolo[4,3,-a]quinoxalin-1-one (ODQ, 10 $\mu\text{mol/l}$).

Finding the optimum "high" glucose concentration. In order to find the highest glucose concentration to mimic the diabetic situation without any effect on cell viability due to hyperosmolarity, we assessed the effect of high glucose and mannitol concentrations on the viability of SH-SY5Y cells. The cells were exposed to varying concentrations of extra glucose or mannitol (0–300 mmol/l) in medium containing 0.5% serum for 24 or 48 h, after serum deprivation for 24 h. The viable cells were then measured using a colorimetric assay based on the ability of live cells to reduce a tetrazolium-based compound to a blue formazan product (MTT method) [23]. At 100 mmol/l or above both glucose and mannitol similarly decreased the viability, suggesting a non-specific effect probably due to hyperosmolarity (not shown). Therefore we used up to 50 mmol/l glucose in our experiments to mimic diabetic conditions.

Immunostaining of SH-SY5Y cells. Cells seeded on glass cover slips were stimulated with RA (25 $\mu\text{mol/l}$) or the vehicle (DM-SO). The cells were then fixed in ice-cold methanol, washed twice in PBS and incubated with nNOS antibody (1:2000; Transduction Laboratories, Oxford, UK) or antibody against a cholinergic nerve marker choline acetyltransferase (ChAT; 1:1000; Chemicon) overnight at 4°C followed by detection with appropriate fluorescent secondary antibodies.

Immunoblotting using SH-SY5Y cells. 2.0×10^7 cells stimulated as above (see Stimulation of SH-SY5Y Cells) were collected, washed and re-suspended in 1 ml of homogenizing buffer [20 mmol/l HEPES, 1 mmol/l EDTA, 0.2 mol/l sucrose, 20 $\mu\text{g/ml}$ soyabean trypsin inhibitor, 20 $\mu\text{g/ml}$ leupeptin, 5 $\mu\text{g/ml}$ pepstatin A, 5 mmol/l DL-dithiothreitol (DTT), 5 $\mu\text{g/ml}$ E-64, 5 $\mu\text{g/ml}$ bestatin, 5 $\mu\text{g/ml}$ aprotinin, 10 $\mu\text{g/ml}$ 3–4-DCL, pH 7.2, 4°C]. The cell membranes were disrupted using a sonicator at 20 μm for 5 s at 4°C. The lysate was centrifuged at 13,000 g for 15 min at 4°C. The protein content of the supernatant was measured and 50 μg of each sample was run on 7.5% polyacrylamide SDS gel and then transferred onto nitrocellulose membranes. The blots were incubated with monoclonal antibodies against nNOS or iNOS (1:500, BD Transduction, Oxford, Oxfordshire, UK) followed by HRP-conjugated anti-mouse IgG (1:4000, Calne, Wiltshire, AutogenBioclear, UK). The reactive bands were detected with a luminol-based kit (ECL, Amersham, Little Chalfont, Buckinghamshire, UK). Cytosols from rat brain or endotoxin-stimulated mouse macrophages (J774) were used as positive controls for nNOS and iNOS respectively.

NOS activity in SH-SY5Y cells. 2×10^7 cells were collected, lysed using HESD buffer (20 mmol/l HEPES pH 7.2, 1 mmol/l EDTA, 0.2 mol/l sucrose, 5 mmol/l dithiothreitol, 0.1 mmol/l PMSF, 20 $\mu\text{g/ml}$ leupeptin and soya bean trypsin inhibitor, 5 $\mu\text{g/ml}$ pepstatin A, E-64, bestatin, aprotinin and 3,4-dichloroisocoumarin) and centrifuged at 13,000 g for 30 min at 4°C. Endogenous L-arginine in the supernatant was removed using activated Dowex-50W resin. Nitric oxide synthase was assayed in the supernatant by the formation of [U-¹⁴C]-citrulline from L-[U-¹⁴C]-arginine as described previously [4].

Measurement of apoptosis. Apoptotic cells were distinguished from non-apoptotic cells by their decreased DNA content as determined by their lower propidium iodide (PI) staining inten-

sity in the presence of RNase. Cells stimulated as above were collected and incubated in the presence of TRIS (10 mmol/l), NaCl (1 mmol/l), RNase (100 $\mu\text{g/ml}$), Tween 20 (0.1%) and PI (0.004%) at 37°C for 25 min. Apoptotic cells were counted using a flow cytometer (FACSCalibur, Becton Dickinson, Oxford, UK).

Caspase-3 assay. 6×10^6 cells stimulated as above were collected and incubated with cell fixation and permeabilization solution (Cytotfix-Cytoperm, BD Biosciences, Oxford, UK) for 15 min at room temperature, washed with wash buffer (Perm-Wash Buffer, BD Biosciences) and incubated with anti-active caspase-3 monoclonal antibody (BD Biosciences) for 1 h at room temperature. The cells were then washed and caspase-3-positive cells were counted using flow cytometry.

NO and ROS. 3-amino-4-aminoethyl-2–7-difluorofluorescein (DAF-FM) and 2–7-dichlorofluorescein diacetate (H₂-DCFDA) were used as fluorescent probes for NO and oxidative stress respectively. They were incubated with 2×10^6 cells at 37°C for 30 min in the presence of 0.5% serum and 0.25 $\mu\text{g/ml}$ PI. The cells were then washed with PBS and the fluorescence signal was measured using flow cytometry.

Statistical analysis. Results are expressed as mean values \pm standard error of the mean from a number (n) of independent experiments or animals. Statistical analyses were performed using Prism software (version 3.0; GraphPad Software, San Diego, Calif., USA). Data were compared by Student's unpaired, two-tailed t -test. A p value of less than 0.05 was considered statistically significant.

Results

Delayed insulin treatment corrects serum glucose and body weight loss. Diabetes was induced in male rats by treating them with STZ. 8 weeks and 12 weeks after STZ injection, some of the animals were implanted with insulin rods (delayed insulin treatment; Groups 20/8, 20/12, 16/4 and 16/8). Some animals received insulin implants immediately after STZ injection (continuous insulin treatment; Groups 20/20, 16/16, 12/12, 8/8 and 4/4). Body weight and serum glucose concentration showed that the untreated diabetic rats lost weight or did not gain as much weight as control animals and their serum glucose concentration remained high. The animals with continuous insulin treatment had similar body weight and serum glucose patterns to control animals. The animals with delayed insulin treatment gained weight and their serum glucose concentrations decreased to non-diabetic levels shortly after implantation of insulin rods (Fig. 1).

Serum AGEs. AGEs concentrations in the serum increased gradually throughout the 20 weeks of diabetes. The slope of the increase was sharper after the 8th week when serum AGEs were measured using fluorometry (Fig. 2a) or after the 12th week when ELISA was used (Fig. 2b). Continuous insulin treatment kept the serum AGEs at control levels (Fig. 2a). Insulin treatment begun at the 8th week did not reduce the

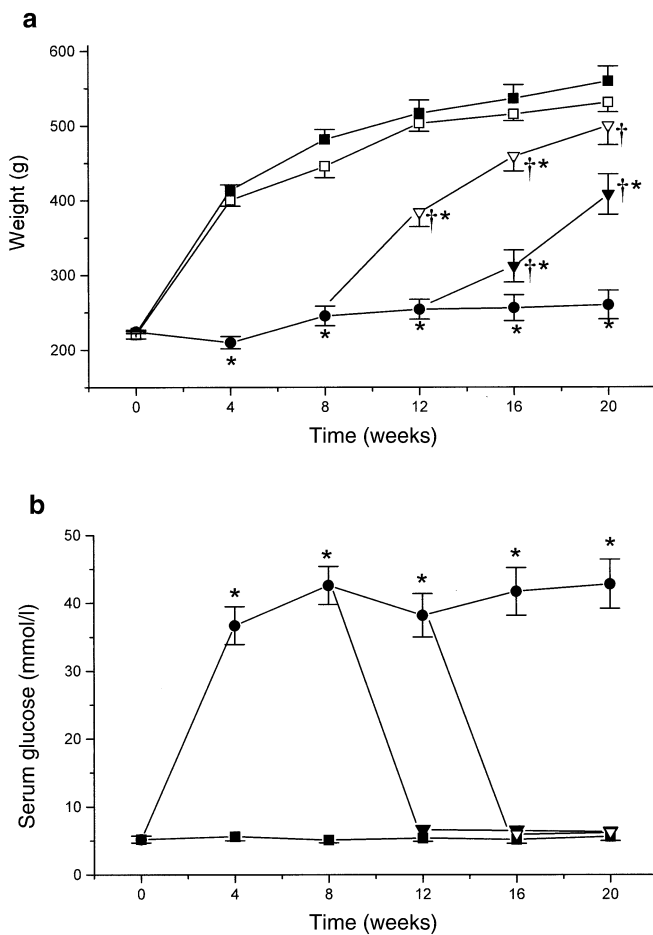


Fig. 1a, b. Body weight (a) and serum glucose concentration (b) of rats at different stages of diabetes. Non-diabetic control animals (filled squares), STZ-treated diabetic animals that received continuous insulin from 0 week (open squares), STZ-treated diabetic animals that received no insulin (filled circles), STZ-treated animals that were implanted with insulin rods at the 8th week (open triangles) and the 12th week (filled triangles). For clarity serum glucose concentrations of diabetic rats which received insulin from 0 week have not been shown; they were similar to the non-diabetic group. * $p < 0.05$ significantly different from control at the same time point. † $p < 0.05$ significantly different from STZ group at the same time point

concentrations of AGEs in the serum but prevented their increase (Fig. 2a,b). Insulin treatment begun at the 12th week, however, failed to prevent the increase in AGEs (Fig. 2a,b).

Accumulation of AGEs in the tissues. AGEs accumulation was evident in the penis, pyloric sphincter (not shown) and MPG (Fig. 2c, Fig. 3) from the 16th week onwards. In the MPG, significant AGE accumulation was observed in both nNOS- and TH-positive cells from the 16th week. Treatment with insulin prevented the accumulation of AGEs in Group 20/12 but not in Group 20/8 (Fig. 2c).

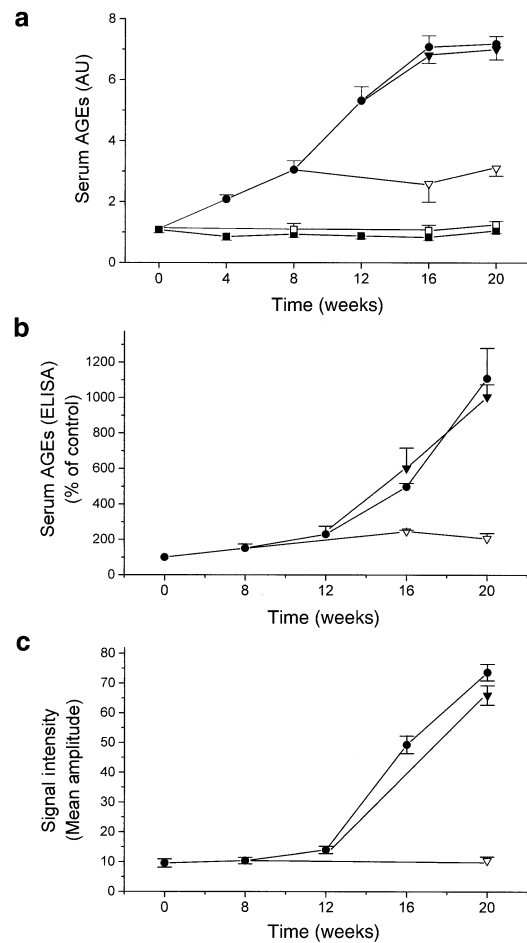


Fig. 2a–c. Serum AGEs and accumulation of AGEs in the MPG. Non-diabetic control animals (filled squares), STZ-treated diabetic animals that received continuous insulin from 0 week (open squares), STZ-treated diabetic animals that received no insulin (filled circles), STZ-treated animals that were implanted with insulin at the 8th week (open triangles) and the 12th week (filled triangles). (a) Serum AGEs, measured as the ratio of AGE-specific-fluorescence to total peptide content, were elevated in STZ-treated animals with a sharp increase after the 8th week, reaching a maximum at the 16th week. (b) Serum AGEs measured using ELISA showed a similar pattern. Insulin treatment begun at the 8th week but not the 12th week prevented further increase in serum AGEs. (c) Immunostaining intensity of AGEs in the MPG showed a sharp increase after the 12th week. * $p < 0.05$ significantly different from control

HSA-AGEs but not high glucose cause apoptosis in nNOS-positive cells. Human neuroblastoma cells (SH-SY5Y) expressed nNOS for 72 h when stimulated with retinoic acid (RA). RA-stimulated cells developed dendritic elongations and were cholinergic (ChAT-positive) (Fig. 4). nNOS protein was detectable by Western blotting for 72 h in RA-treated cells but not in control cells (not shown) and constitutive NOS activity was increased following RA stimulation from undetectable levels to 400 fmol/mg protein/min. There was no detectable inducible NOS protein or activity in the cells with or without RA-stimulation (not shown). Therefore we used control (untreated) SH-SY5Y cells

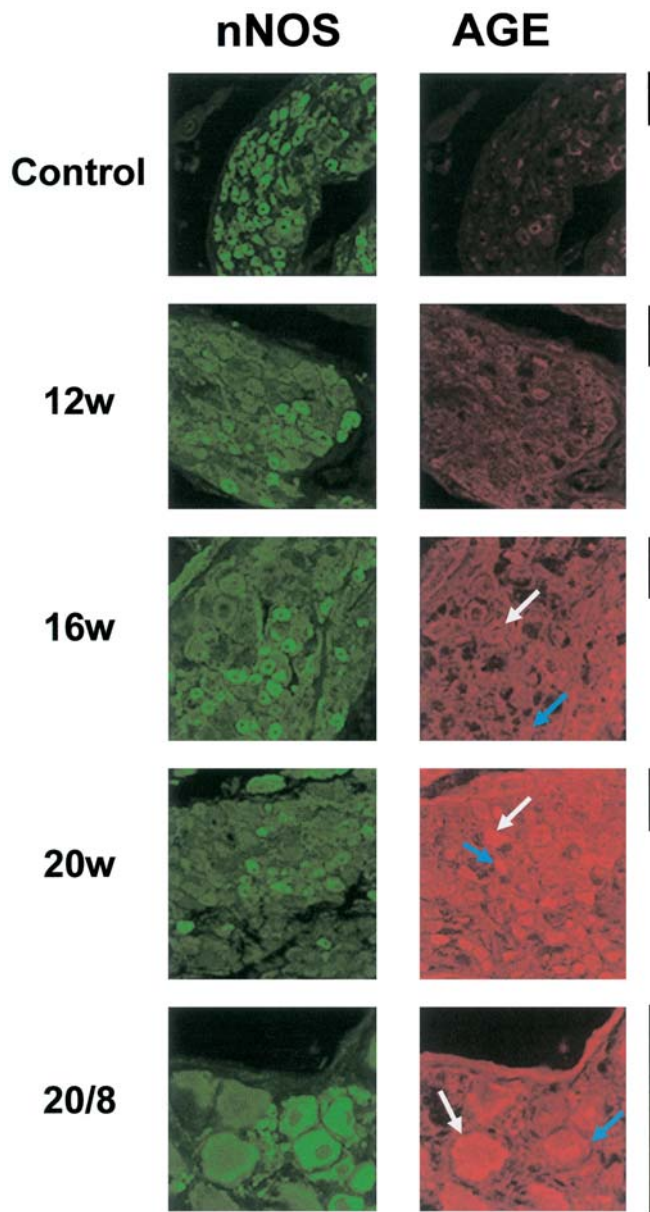


Fig. 3. Accumulation of AGEs was evident in the MPG by the 16th week. nNOS-positive (*blue arrow*) and nNOS-negative cells (*white arrow*) were equally immunostained with anti-AGE-antibody. Scalebar is 120 μ

and RA-treated SH-SY5Y cells as a nNOS-negative and nNOS-positive peripheral nerve cell model, respectively.

When exposed to HSA-AGEs (0.5 mg/ml), the SH-SY5Y cells underwent apoptosis. The percentage of apoptotic cells was significantly higher in RA-treated and AGE-treated cells than in controls. However RA and AGEs in combination caused more apoptosis than either did alone. The combination of RA and AGEs was supra-additive at 48 and 72 h. Synergistic action of RA and AGEs was prevented if the cells were treated with L-NAME, Z-VAD-FMK, sRAGE or NAC but not ODQ (Fig. 5, Fig. 6). High glucose (50 mmol/l)

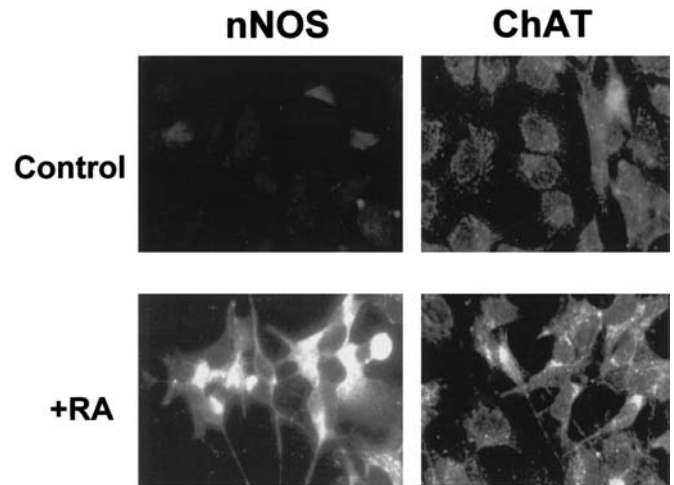


Fig. 4. Effect of retinoic acid (RA) on the human neuroblastoma SH-SY5Y cells. Treatment with RA increases nNOS and choline acetyl transferase (ChAT) expression and induces dendritic elongation in SH-SY5Y cells

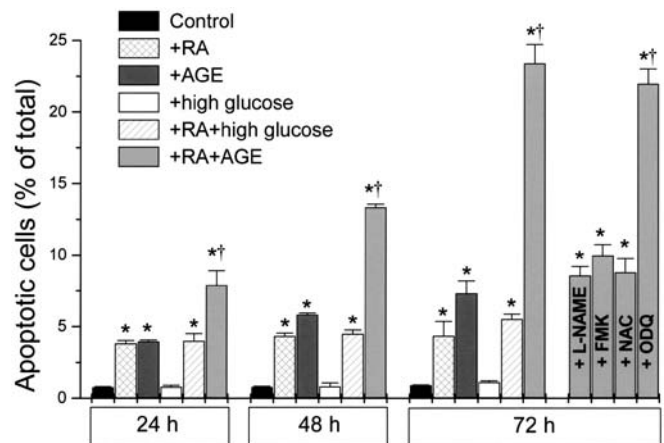


Fig. 5. In SH-SY5Y cells HSA-AGEs induce apoptosis, which is augmented with endogenous NO. The percentage of apoptotic cells increased more in the groups with RA+HSA-AGE than with RA or HSA-AGEs alone. This was prevented when the cells were treated with the NOS inhibitor, L-NAME (500 μ mol/l), the pan-caspase inhibitor Z-VAD-FMK (FMK; 50 μ mol/l) or the anti-oxidant N-acetyl-L-cysteine (NAC; 100 μ mol/l) but not with an inhibitor of soluble guanylate cyclase (ODQ; 10 μ mol/l). * p <0.05 significantly different from control; † p <0.05 significantly different from other treatments in the same group

did not increase apoptosis in the absence or presence of RA-stimulation (Fig. 5).

HSA-AGEs-induced apoptosis is caspase-3-dependent. The percentage of caspase-3-positive cells increased significantly when RA-stimulated cells were exposed to HSA-AGEs; this was prevented if the cells were pre-treated with L-NAME, Z-VAD-FMK or NAC but not with ODQ. RA alone or HSA-AGEs alone were equally effective in increasing caspase-3-positive cells but were more effective in combination

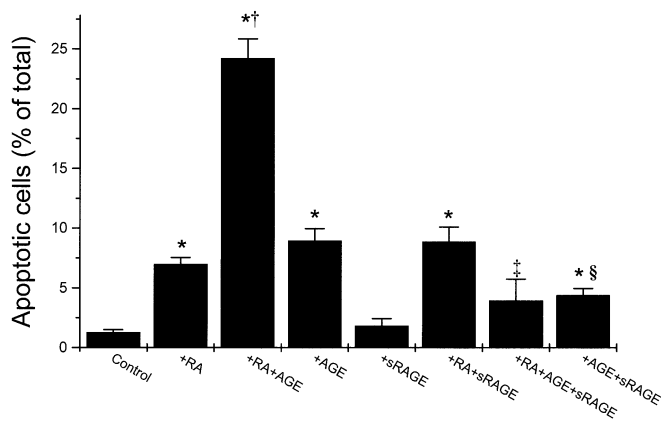


Fig. 6. Treatment of cells with soluble receptor of AGEs (sRAGE) prevents apoptosis induced by HSA-AGEs. sRAGE (125 µg/ml) prevented apoptotic cell death induced by HSA-AGEs alone or RA+HSA-AGEs but not by RA alone. * $p < 0.05$ significantly different from control; † $p < 0.05$ significantly different from other treatments; ‡ $p < 0.05$ significantly different from RA+AGE; § $p < 0.05$ significantly different from AGE only

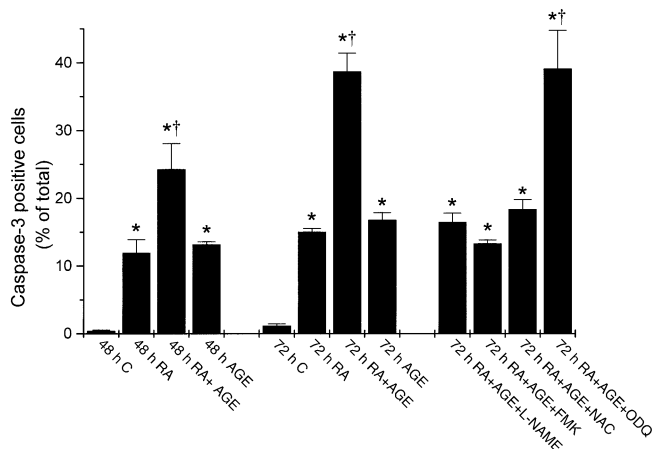


Fig. 7. HSA-AGEs-induced apoptosis in nNOS-positive cells is caspase-3-dependent. Caspase-3-positive cells increased in number more in the RA+HSA-AGEs group than in the RA or HSA-AGEs groups alone. L-NAME, Z-VAD-FMK, NAC but not ODQ reversed this. * $p < 0.05$ significantly different from control; † $p < 0.05$ significantly different from other treatments in the same group

(Fig. 7). High glucose did not affect the caspase-3 positivity in any group (not shown).

Combination of AGEs and endogenous NO induces oxidative stress. We measured NO and reactive oxygen species (ROS) in SH-SY5Y cells using intracellular fluorescent probes. The NO signal was increased by RA or RA+HSA-AGEs but not by HSA-AGEs alone. The ROS signal was increased by RA+HSA-AGEs or HSA-AGEs alone. The highest increase in ROS was found in the RA+HSA-AGE group. The increase in the NO and ROS signals in RA+HSA-AGE group was attenuated in the presence of L-NAME. L-NAME did not affect the ROS signal when the cells

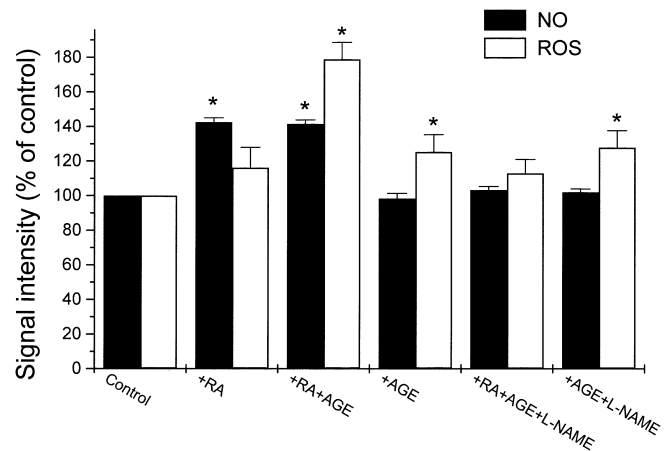


Fig. 8. HSA-AGEs-induced apoptosis in nNOS-positive cells is associated with increased oxidative stress. Reactive oxygen species (ROS; white columns) and NO (black columns) were measured in SH-SY5Y cells using intracellular fluorescent probes (H₂-DCFDA and DAF-FM respectively). * $p < 0.05$ significantly different from control

were exposed to AGEs alone (Fig. 8). High glucose concentrations (up to 50 mmol/l) did not increase NO or ROS signal in any group (not shown).

Discussion

We observed a gradual increase in serum AGEs concentration throughout the 20 weeks of diabetes. However after the 8th–12th week a sharper increase was detected. The reasons for this are not clear, although it is possible that the clearance mechanisms for AGEs were impaired as diabetes progressed [24, 25]. This is also suggested by the fact that in STZ-diabetic animals early insulin treatment (started at the 8th week) prevented a further increase in AGEs while the delayed treatment (started at the 12th week) failed completely to prevent it. Interestingly, accumulation of AGEs in tissues could only be detected after 12 weeks of diabetes. Together, these results suggest that the AGEs formed early on are adequately cleared from the plasma and tissue compartments and that this clearing mechanism is impaired as the disease progresses. Furthermore, our results seem to indicate that a critical concentration of AGEs in the plasma is necessary for AGEs accumulation in the tissues and subsequent tissue damage to occur. It is also likely that accumulation of AGEs in tissues explains the progression of hyperglycaemia-induced alterations during normal glucose homeostasis [26, 27]. Indeed, in our delayed insulin treatment group (group 20/8) serum AGEs were high and there was accumulation of AGEs in the MPG even though serum glucose concentrations had been normalized. Moreover we have observed neuronal apoptosis in vivo in the nitrergic neurons in this group [16].

Since the steep increase in serum AGEs and accumulation of AGEs in the tissues coincided with apoptosis which occurred selectively in the nitrergic neurons of STZ-induced diabetic rats [16], we hypothesized that the combination of endogenous NO and AGEs could be the cause of the selective nitrergic cell death leading to nitrergic nerve fibre loss. In order to test this hypothesis we exposed undifferentiated and differentiated SH-SY5Y human neuroblastoma cells, which are nNOS-negative and positive respectively, to exogenous HSA-AGEs. HSA-AGEs alone produced caspase-3-dependent apoptotic cell death, in accordance with previous studies [28, 29]. HSA-AGEs-induced apoptosis was significantly increased in the nNOS-positive cells; this could be prevented if the cells were treated with an inhibitor of NOS, suggesting a synergistic action of AGEs and NO in inducing apoptosis.

Apoptosis due to HSA-AGEs in the nNOS-positive cells was not inhibited by ODQ, showing that this is not a process dependent on activation of soluble guanylyl cyclase. However, it could be prevented by treatment with an antioxidant, pointing to oxidative stress as a cause of cell death. Since AGEs and oxidative stress have been linked [30] and endogenous NO is known to contribute to intracellular oxidative stress [31], we investigated oxidative stress markers in SH-SY5Y cells. Indeed we have found that the highest increase in ROS upon exposure to AGEs occurred in nNOS-positive cells.

The induction of cell death by both AGEs and NO has been associated previously with oxidative stress [32, 33, 34, 35]. The source of oxidative stress in diabetes mellitus, however, has not been fully elucidated. In endothelial cells, hyperglycaemia-induced overproduction of superoxide has been claimed to activate the hexosamine pathway and lead to the formation of intracellular AGEs [36]. Similarly, hyperglycaemic conditions have been linked to oxidative stress and induction of neuronal apoptosis [37]. In both of the above studies hyperglycaemia-induced mitochondrial dysfunction has been suggested to be the source of ROS. However, in our studies we could not observe either apoptosis or ROS formation in the presence of high concentrations of glucose. Our results suggest that AGEs rather than hyperglycemia per se are a prerequisite for ROS formation and cell death.

Whether AGEs induce ROS formation directly [38] or through their receptor, RAGE [34] has been debated. We think that in our experiments ROS are generated through RAGE because of two reasons: Firstly, the measurement of ROS was performed after AGEs were removed from the medium, suggesting that an intracellular mechanism of ROS formation must have been switched on by AGEs, most probably through RAGE. Secondly, co-incubation of AGEs with sRAGE prevented the cells from undergoing apoptosis. Further research would be required to investigate

the intracellular pathway involved in ROS formation following RAGE activation.

Aminoguanidine, a potent inhibitor of AGE-mediated crosslinking, has been shown to prevent the development of nitrergic dysfunction in the penis [39, 40] and to prevent depletion of nitrergic neurones in the retina of diabetic rats [41]. However aminoguanidine also inhibits nNOS [42] and iNOS [43]. New compounds which inhibit formation of AGEs, break the AGE-crosslink or inhibit RAGE without affecting NO synthesis [44] need to be evaluated in prevention of nitrergic neuropathy.

Our *in vitro* (present study) and *in vivo* results [16] indicate a role for endogenous NO produced by nNOS in apoptotic cell death. Other forms of NOS which could be involved in the apoptotic process by producing high amounts of NO are inducible NOS (iNOS) and endothelial NOS (eNOS). In our studies, however, we did not detect induction of iNOS in the penis or pyloric sphincter of diabetic rats or in the SH-SY5Y cells when exposed to RA or AGEs (S. Cellek, unpublished observations). Peroxynitrite, the product of the reaction between NO and superoxide in arterioles that provide circulation to the sciatic nerve, has been suggested to be involved in diabetic neuropathy [45, 46]. Although we did not detect any increase in nitrotyrosine immunostaining in diabetic rat penis [4], we cannot exclude the possibility that eNOS from nearby blood vessels could produce NO, leading to nitrergic degeneration. Therefore we suggest that endogenous NO derived from nNOS in the nitrergic neurones and/or eNOS in the nearby endothelial cells is involved in the apoptotic death of neurones.

We could not detect any difference between AGEs accumulation in neurons which die earlier (i.e. nitrergic/cholinergic nerves which are nNOS-positive) and those which die later (i.e. sympathetic which are TH-positive and nNOS-negative) in the course of diabetes. AGEs seem to be accumulating equally in every compartment of the ganglia without any preference. The difference between early and late death seems to be determined by the presence of NO within the cell. Indeed, nitrergic nerves seem to be more sensitive to diabetic insult than sympathetic nerves which do not contain nNOS [4, 16]. Therefore we propose that the synergistic action of extracellular AGEs and endogenous NO within the nitrergic neuron leads to selective nitrergic degeneration in diabetes.

In conclusion the results of the present study show an increase in serum AGEs during diabetes that cannot be reversed after a certain time point by insulin treatment. Furthermore, exogenous application of HSA-AGEs to differentiated human neuroblastoma cells induces NO- and caspase-3-dependent apoptosis which involves increased oxidative stress. These results suggest a pivotal role for AGEs and NO in the pathogenesis of diabetic autonomic neuropathy.

Acknowledgements. S. Cellek is a fellow of the Juvenile Diabetes Research Foundation International (JDRF) and this work is supported by the JDRF. The authors thank A. Higgs, D. Goodwin, A. Alvarez, L. Martinez and D. Campbell for their help.

References

1. Saenz de Tejada I, Goldstein I, Azadzi K, Krane RJ, Cohen RA (1989) Impaired neurogenic and endothelium-mediated relaxation of penile smooth muscle from diabetic men with impotence. *N Engl J Med* 320:1025–1030
2. Azadzi KM, Saenz de Tejada I (1992) Diabetes mellitus impairs neurogenic and endothelium-dependent relaxation of rabbit corpus cavernosum smooth muscle. *J Urol* 148:1587–1591
3. Jenkinson KM, Reid JJ (1995) Effect of diabetes on relaxations to non-adrenergic, non-cholinergic nerve stimulation in longitudinal muscle of rat gastric fundus. *Br J Pharmacol* 116:1551–1556
4. Cellek S, Rodrigo J, Lobos E, Fernández P, Serrano J, Moncada S (1999) Selective nitrenergic neurodegeneration in diabetes mellitus- a nitric oxide-dependent phenomenon. *Br J Pharmacol* 128:1804–1812
5. Watkins CC, Sawa A, Jaffrey S, Blackshaw S, Barrow RK, Snyder SH, Ferris, CD (2000) Insulin restores neuronal nitric oxide synthase expression and function that is lost in diabetic gastropathy. *J Clin Invest* 106:373–384
6. He C-L, Soffer EE, Ferris CD, Walsh RM, Szurszewski JH, Farrugia G (2001) Loss of interstitial cells of Cajal and inhibitory innervation in insulin-dependent diabetes. *Gastroenterology* 121:427–434
7. Giraldi A, Persson K, Werkstrom V, Alm P, Wagner G, Andersson KE (2001) Effects of diabetes on neurotransmission in rat vaginal smooth muscle. *Int J Impot Res* 13:58–66
8. Vernet D, Cai L, Garban H, Babbitt ML, Murray FT, Rajfer J, Gonzalez-Cadavid NF (1995) Reduction of penile nitric oxide synthase in diabetic BB/WOR^{dp} (Type I) and BBZ/WOR^{dp} (Type II) rats with erectile dysfunction. *Endocrinology* 136:5709–5717
9. Rehman J, Chenven E, Brink P, Peterson B, Walcott W, Wen YP, Melman A, Christ G (1997) Diminished neurogenic but not pharmacological erections in the 2- to 3-month experimentally diabetic F-344 rat. *Am J Physiol* 272:H1960–H1971
10. Wrzos HF, Cruz A, Polavarapu R, Shearer D, Ouyang A (1997) Nitric oxide synthase expression in the myenteric plexus of streptozotocin-diabetic rats. *Dig Dis Sci* 42:2106–2110
11. El-Sakka AI, Lin C-S, Chui RM, Dahiya R, Lue TF (1999) Effects of diabetes in nitric oxide synthase and growth factor genes and protein expression in an animal model. *Int J Impot Res* 11:123–132
12. Way KJ, Reid JJ (1999) Insulin reversal of impaired nitrenergic transmission in the anococcygeus muscle from diabetic rats. *Pharmacol* 59:115–126
13. Podlasek CA, Zelner DJ, Bervig TR, Gonzalez CM, McKenna KE, McVary KT (2001) Characterization and localization of nitric oxide synthase isoforms in the BB/WOR diabetic rat. *J Urol* 166:746–755
14. Escrig A, Marin R, Abreu P, Gonzalez-Mora JL, Mas M (2002) Changes in mating behaviour, erectile function, and nitric oxide levels in penile corpora cavernosa in streptozotocin-diabetic rats. *Biol Reprod* 66:185–189
15. Shotton HR, Clarke S, Lincoln J (2003) The effectiveness of treatments of diabetic autonomic neuropathy is not the same in autonomic nerves supplying different organs. *Diabetes* 52:157–164
16. Cellek S, Foxwell AN, Moncada S (2003) Two phases of nitrenergic neuropathy in streptozotocin-induced diabetic rats. *Diabetes* 52:2353–2362
17. Brownlee M (1991) Glycosylation products as toxic mediators of diabetic complications. *Annu Rev Med* 42:159–166
18. Wolffenbuttel BH, Giordano D, Founds HW, Bucala R (1996) Long-term assessment of glucose control by haemoglobin-AGE measurement. *Lancet* 347:513–515
19. Mañas-Rodríguez L, Angulo J, Vallejo S, Peiró C, Sánchez-Ferrer A, Cercas E, López-Dóriga P, Sánchez-Ferrer CF (2003) Early and intermediate Amadori glycosylation adducts, oxidative stress and endothelial dysfunction in the streptozotocin-induced diabetic rat vasculature. *Diabetologia* 46:556–566
20. Wróbel K, Wróbel K, Sevilla MEG, Nava LE, Malacara JM (1997) Novel analytical approach to monitoring advanced glycosylation end products in human serum with on-line spectrophotometric and spectrofluorometric detection in a flow system. *Clin Chem* 43:1563–1569
21. Zilin S, Naifeng L, Bicheng L, Jiping W (2001) The determination of AGE-peptides by flow injection assay, a practical marker of diabetic nephropathy. *Clin Chim Acta* 313:69–75
22. Herbison AE, Simonian SX, Norris PJ, Emson PC (1996) Relationship of neuronal nitric oxide synthase immunoreactivity to GnRH neurons in the ovariectomized and intact female rat. *J Neuroendocrinol* 8:73–82
23. Mosmann T (1983) Rapid colorimetric assay for cellular growth and survival. *J Immunol Methods* 65:55–63
24. Sebekova K, Podracka L, Blazicek P, Syrova D, Heidland A, Schinzel R (2001) Plasma levels of advanced glycation end products in children with renal disease. *Pediatr Nephrol* 16:1105–1112
25. Niwa T, Miyazaki T, Katsuzaki T, Tatemichi N, Takei Y (1996) Serum levels of 3-deoxyglucosone and tissue contents of advanced glycation endproducts are increased in streptozotocin-induced diabetic rats with nephropathy. *Nephron* 74:580–585
26. Engerman RL, Kern TS (1987) Progression of incipient diabetic retinopathy during good glycemic control. *Diabetes* 36:808–812
27. Brownlee M (2001) Biochemistry and molecular cell biology of diabetic complications. *Nature* 414:813–820
28. Min C, Kang E, Yu SH, Shinn SH, Kim YS (1999) Advanced glycation end products induce apoptosis and procoagulant activity in cultured human umbilical vein endothelial cells. *Diabetes Res Clin Pract* 46:197–202
29. Yamagishi S, Amano S, Inagaki Y, Okamoto T, Koga K, Sasaki N, Yamamoto H, Takeuchi M, Makita Z (2002) Advanced glycation end products-induced apoptosis and overexpression of vascular endothelial growth factor in bovine retinal pericytes. *Biochem Biophys Res Commun* 290:973–978
30. Loske C, Neumann A, Cunningham AM, Nichol K, Schinzel R, Riederer P, Münch G (1998) Cytotoxicity of advanced glycation endproducts is mediated by oxidative stress. *J Neural Transm* 105:1005–1015
31. Moncada S, Erusalimsky JD (2002) Does nitric oxide modulate mitochondrial energy generation and apoptosis? *Nature Rev Mol Cell Biol* 3:214–220
32. Uehara T, Kikuchi Y, Nomura Y (1999) Caspase activation accompanying cytochrome c release from mitochondria is possibly involved in nitric oxide-induced neuronal apoptosis in SH-SY5Y cells. *J Neurochem* 72:196–205
33. Deuther-Conrad W, Loske C, Schinzel R, Dringen R, Riederer P, Münch G (2001) Advanced glycation endprod-

- ucts change glutathione redox status in SH-SY5Y cells by a hydrogen peroxide dependent mechanism. *Neurosci Lett* 312:29–32
34. Wautier MP, Chappey O, Corda S, Stern DM, Schmidt AM, Wautier JL (2001) Activation of NADPH oxidase by AGE links oxidant stress to altered gene expression via RAGE. *Am J Physiol Endocrinol Metab* 280:E685–E694
 35. Vincent AM, Brownlee M, Russell JW (2002) Oxidative stress and programmed cell death in diabetic neuropathy. *Ann NY Acad Sci* 959:368–383
 36. Nishikawa T, Edelstein D, Du XL, Yamagishi S, Matsumura T, Kaneda Y, Yorek MA, Beebe D, Oates PJ, Hammes HP, Giardino I, Brownlee M (2000) Normalizing mitochondrial superoxide production blocks three pathways of hyperglycaemic damage. *Nature* 404:787–790
 37. Russell JW, Sullivan KA, Windebank AJ, Herrmann DN, Feldman EL (1999) Neurons undergo apoptosis in animal and cell culture models of diabetes. *Neurobiol Dis* 6:347–363
 38. Mullarky CJ, Edelstein D, Brownlee M (1990) Free radical generation by early glycation products: a mechanism for accelerated atherogenesis in diabetes. *Biochem Biophys Res Commun* 173:932–939
 39. Cartledge JJ, Eardley I, Morrison JF (2001) Advanced glycation end-products are responsible for the impairment of corpus cavernosal smooth muscle relaxation seen in diabetes. *BJU Int* 87:402–407
 40. Usta MF, Bivalacqua Tj, Yang DY, Ramanitharan A, Sell DR, Viswanathan A, Monnier VM, Hellstrom WJG (2003) The protective effect of aminoguanidine on erectile function in streptozotocin diabetic rats. *J Urol* 170:1437–1442
 41. Roufail E, Soulis T, Boel E, Cooper ME, Rees S (1998) Depletion of nitric oxide synthase-containing neurons in the diabetic retina: reversal by aminoguanidine. *Diabetologia* 41:1419–1425
 42. Jianmongkol S, Vuletich JL, Bender AT, Demady DR, Osawa Y (2000) Aminoguanidine-mediated inactivation and alteration of neuronal nitric oxide synthase. *J Biol Chem* 275:13370–13376
 43. Misko TP, Moore WM, Kasten TP, Nickols GA, Corbett JA, Tilton R, McDaniel ML, Williamson JR, Currie MG (1993) Selective inhibition of the inducible nitric oxide synthase by aminoguanidine. *Eur J Pharmacol* 233:119–125
 44. Stitt AW, Jenkins AJ, Cooper ME (2002) Advanced glycation end products and diabetic complications. *Expert Opin Investig Drugs* 11:1205–1223
 45. Coppey LJ, Davidson EP, Dunlap JA, Lund DD, Yorek MA (2000) Slowing of motor nerve conduction velocity in streptozotocin-induced diabetic rats is preceded by impaired vasodilation in arterioles that overlie the sciatic nerve. *Int J Exp Diabetes Res* 1:131–143
 46. Coppey LJ, Gellett JS, Davidson EP, Dunlap JA, Lund DD, Yorek MA (2001) Effect of antioxidant treatment of streptozotocin-induced diabetic rats on endoneurial blood flow, motor nerve conduction velocity, and vascular reactivity of epineurial arterioles of the sciatic nerve. *Diabetes* 50:1927–1937